4-(cyanomethyl)anilinium Perchlorate: A New Displacive-Type Molecular Ferroelectric

Hong-Ling Cai,[1] Wen Zhang,[1,*] Jia-Zhen Ge,[1] Yi Zhang,[1] Kunio Awaga,[2] Takayoshi Nakamura,[3] and Ren-Gen Xiong[1,†]

[1]*Ordered Matter Science Research Center, Southeast University, Nanjing 211189, People's Republic of China*

[2]*Research Center for Materials Science and Department of Chemistry, Nagoya University, Nagoya, Japan*

[3]*Research Institute for Electronic Science, Hokkaido University, Sapporo, Japan*

(Received 8 May 2011; published 28 September 2011)

A new organic ferroelectric compound, 4-(cyanomethyl)anilinium perchlorate, proceeds a second-order phase transition from a paraelectric phase ($P2_1/m$) to a ferroelectric phase ($P2_1$) at 184 K. A perfect ferroelectric hysteresis loop was observed even at 10 KHz. It is the first example of a molecule-based organic ferroelectric whose polarization can be switched at such a high frequency. The temperature dependent second harmonic generation effect shows that the second-order nonlinear coefficient is nearly zero above T_c and proportional to the spontaneous polarization below T_c, suggesting the occurrence of symmetry breaking, in good agreement with crystal structural determination. The origin of ferroelectricity was ascribed to the displacements of $-NH_3^+$ cations and ClO_4^- anions from the symmetric positions including a small part of the order-disorder behaviors of the ClO_4^- anions.

DOI: 10.1103/PhysRevLett.107.147601 PACS numbers: 77.84.Jd, 42.65.Ky, 61.50.Ks, 65.40.Ba

Ferroelectric materials are characterized by a spontaneous electrical polarization which can be reversed by an applied electric field. They are very useful in the fields of ferroelectric random access memory (FeRAM), capacitors, piezoelectric devices, and nonlinear optical devices [1,2]. Most commercial ferroelectrics belong to inorganic ceramics of the perovskite family such as barium titanate [$BaTiO_3$ (BTO)] and lead zirconate titanate [$Pb(Zr_xTi_{1-x})O_3$]. Because of the difficulties in the utilization of toxic and expensive heavy metals, high-temperature processing, and growth of large single crystals, development of high-performance molecular ferroelectrics is urgently needed to overcome the above mentioned drawbacks [3–7].

Ferroelectric polymers and organic molecular materials are therefore highly desirable because they are soluble in organic solvents and amenable to low-temperature fabrication techniques. Recently, Horiuchi *et al.* [8] have reported that the crystal of croconic acid displays a high polarization of 22 $\mu C \cdot cm^{-2}$ at a very low frequency of 1 Hz, requires a low operating voltage, and retains the ferroelectricity up to 130 °C. However, the very low working frequency limits its application in FeRAM, which needs a relatively fast polarization switch (normally nanosecond range). As we are aware, there are still no organic and polymeric ferroelectrics, which display a good ferroelectric hysteresis loop at high frequencies. A lot of research focuses on molecule-based ferroelectrics only at very low frequencies such as $[Hdabco]^+A^-$ (dabco = 1, 4-diazabicyclo[2.2.2]octane) at 50 Hz [9–11] and at 400 Hz [12], $[C(NH_2)_3]_4X_2SO_4$ (X = Cl or Br) at 50 Hz [13,14], $[C_3N_2H_5]_5[Bi_2Cl_{11}]$ and $[C_3N_2H_5]_5[Sb_2Br_{11}]$ at 50 Hz [15,16], $Co^{II}Cl_3$(H-MPPA) at 50 Hz [17], $[H_2\text{-TPPZ}][Hxa]_2$ (TPPZ = 2, 3, 5, 6-tetra (2-pyridyl)pyrazine, H_{xa} = chloranilate or = bromanilate) at 1 Hz [18], and Phz-H_2xa [Phz-H_2xa(Phz = phenazine)]at 10 Hz [19].

Herein we report the synthesis and characterizations of a new organic ferroelectric compound, 4-(cyanomethyl) anilinium perchlorate (CMAP). Its ferroelectricity was well confirmed by variable-temperature crystal structures, thermal analyses including differential scanning calorimetry (DSC), and specific heat capacity (HC), second harmonic generation (SHG), anisotropic dielectric anomalies, and ferroelectric hysteresis loops. To the best of our knowledge, CMAP is the first example of molecule-based ferroelectrics exhibiting good ferroelectric hysteresis loop even at a relatively high frequency of 10 kHz.

CMAP crystallizes in a monoclinic crystal system with a space group of $P2_1/m$ at 293 K and still in a monoclinic crystal system but with a space group of $P2_1$ at 93 K (Fig. 1). The number of symmetric operation elements decreases from four (1, 2, $\bar{1}$, and m) to two (1 and 2) during the process of cooling. It is clear that $P2_1$ is a subgroup of $P2_1/m$, which is consistent with the condition of the second-order phase transition of the Landau theory.

In order to confirm the second-order phase transition, thermal analyses were performed. It is known that during a first-order phase transition process, a system either absorbs or releases a fixed latent heat, which displays a very sharp peak in a HC curve. However, the HC curve of CMAP exhibits a broad peak at about 185 K and a very little heat hysteresis of about 2 K [Fig. 2(a)], which is a characteristic of a second-order transition. Assuming a smooth base line of the HC curve, an entropy change ΔS is estimated with a value of 0.763 $J\,K^{-1}\,mol^{-1}$. Given that $\Delta S = R \ln g$, where g represents the ratio of possible configurations and R is the gas constant, it is found that $g = 1.096$. In DSC measurements [Fig. 2(a)], a pair of broad peaks was found in the temperature range of 170–200 K during cooling and

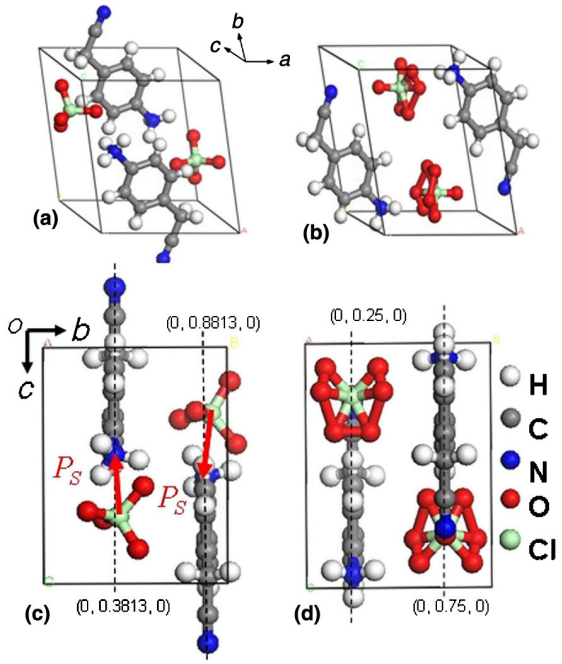

FIG. 1 (color online). Crystal structures of CMAP at 93 K [(a) and (c)] and 293 K [(b) and (d)]. (a) and (b) are 3-dimensional pictures. (c) and (d) are viewed from the [100] direction in order to observe clearly the spontaneous polarization. At 293 K (d), there is no remnant polarization since all the chlorine and nitrogen atoms are located at the (0, 0.25, 0) and (0, 0.75, 0) planes. At 93 K (c), a polarization shown as an arrow occurs due to symmetry breaking.

heating processes, indicating a continuous phase transition as shown in the HC experiment. The estimated ΔS is 0.915 $\mathrm{J\,K^{-1}\,mol^{-1}}$ and $g = 1.116$, which is consistent with the HC measurement.

The disorder of the $-NH_3^+$ cation and ClO_4^- anion may be statistical or dynamic. In order to check if the disorder is dynamic, dielectric measurements were performed on single crystals of CMAP. The real part of the complex dielectric constant increases from 10 to about 1300 during the phase transition process, corresponding to an enhancement of about 2 orders of magnitude [Fig. 2(b)]. The behavior of the temperature dependence of dielectric constants both in ferroelectric and paraelectric phases can be well fitted with the Curie-Weiss law, $\varepsilon = C/(T - T_0)$, where C is the Curie-Weiss constant and T_0 is the Curie temperature [inset of Fig. 2(b)]. The fitted parameters are tabulated in the Supplemental Materials [20]. It is found that the value of T_0 decreases with the increase of frequency and it is almost equal to the T_c at 1 MHz, suggesting that the phase transition should be a second-order transition. The C_{para} increases while the C_{ferro} decreases with frequency increasing. The ratio of C_{para} to C_{ferro} is in the range of 1.2–1.9 and smaller than 4, suggesting that this phase transition should be second order.

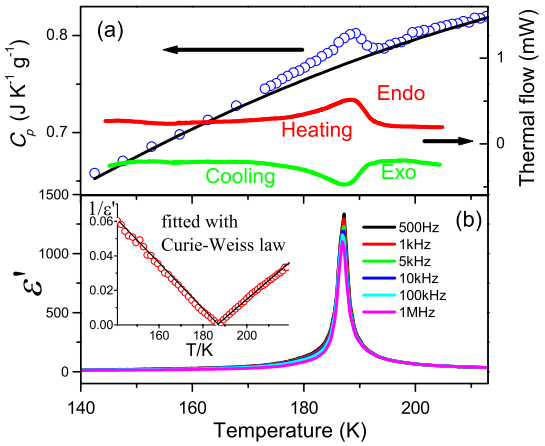

FIG. 2 (color online). The temperature dependence of the (a) specific heat capacity and DSC and (b) dielectric constant at different frequencies. The inset of (b) shows a linear fit to the Curie-Weiss law at a frequency of 500 Hz.

One of the most important characteristics of ferroelectrics is the ferroelectric hysteresis loop. Therefore, the polarization as a function of the electric field was performed at different temperatures and frequencies. At 188 K (above the T_c), P-E curve is nearly a linear line without any hysteresis, while below the T_c it shows a standard hysteresis loops [Fig. 3(a)]. Particularly, a perfect ferroelectric hysteresis loop was observed at a frequency even as high as 10 KHz below T_c [Fig. 3(b)]. It opens up a new application in FeRAM. The operating frequencies of previously reported organic ferroelectrics do not exceed 500 Hz [8–18], probably due to the fact that they are order-disorder–type ferroelectrics. The reason why the operating frequency of CMAP exceeds 10 KHz is ascribed to the fact that the ferroelectricity of CMAP mainly comes from displacive-type, as discussed below.

This second-order paraelectric-ferroelectric phase transition can be well described by the Landau theory. Based on the Aizu notation $2/mF2$, we conclude the polar direction is along the b axis, and then $P_x = P_z = 0$. Hence, the Gibbs free energy based on Landau theory is written as below:

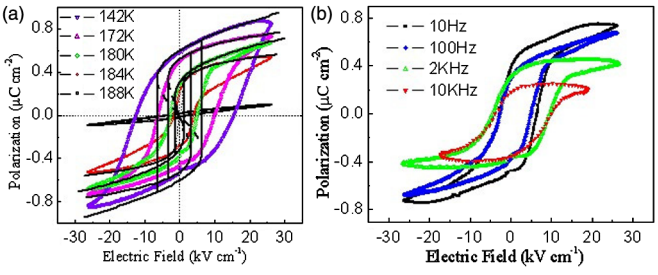

FIG. 3 (color online). The ferroelectric hysteresis loops at (a) different temperatures with a frequency of 100 Hz and (b) different frequencies with a temperature of 180 K. The solid lines in (a) are fitted curves using Landau theory.

$$G_1 = G_0 + \tfrac{1}{2}\alpha P_y^2 + \tfrac{1}{4}\beta P_y^4 + \tfrac{1}{6}\gamma P_y^6 + \cdots, \quad (1)$$

where α is linearly correlated with the temperature factor, $\alpha = \alpha_0(T - T_c)$. When an external electric field applied, the Gibbs free energy should be written as

$$G_1 = G_0 + \tfrac{1}{2}\alpha P_y^2 + \tfrac{1}{4}\beta P_y^4 + \tfrac{1}{6}\gamma P_y^6 - EP_y, \quad (2)$$

where E is the applied electric field. Thus, the free energy reaches its extreme value when

$$\frac{\partial G_1}{\partial P_y} = \alpha P_y + \beta P_y^3 + \gamma P_y^5 - E = 0. \quad (3)$$

The fitted hysteresis loops are shown in Fig. 3(a) as solid lines, which are well consistent with the experimental results.

Since $\partial G_1/\partial D = E$, $\partial^2 G_1/\partial D^2 = 1/\varepsilon$, the entropy of the system should be defined as $S = -(\partial G_1/\partial T)_{X,D}$. Thus, the entropy change should be estimated as $\Delta S = S_0 - S = -(\partial G_{10}/\partial T)_{X,D} + (\partial G_1/\partial T)_{X,D}$. When the phase transition occurs, noting that $E = 0$, $D = P_y = P_s$, according to Eq. (1), the entropy change should be

$$\Delta S = \frac{1}{2}P_s^2\frac{\partial[\alpha_0(T - T_0)]}{\partial T} + \frac{1}{4}P_s^4\frac{\partial \beta}{\partial T} + \frac{1}{6}P_s^6\frac{\partial \gamma}{\partial T}. \quad (4)$$

If ignoring the change of β and γ with the temperature, the entropy change can be written as $\Delta S = \frac{1}{2}\alpha_0 P_s^2$. Since $\alpha_0 = 1/(\varepsilon_0 C)$, we get the spontaneous polarization P_s as

$$P_s = (\Delta S \times 2\varepsilon_0 C)^{1/2}. \quad (5)$$

Based on this formula, the values of the P_s are calculated as 0.90 $\mu C \cdot cm^{-2}$ from the HC data and 0.99 $\mu C \cdot cm^{-2}$ from the DSC data, showing a good agreement with each other. The measured P_s equals 0.75 $\mu C \cdot cm^{-2}$, slightly smaller than the calculated values, probably suggesting that the ferroelectric polar axis slightly deviates from the polar b axis. Notably, around the T_c, the change of spontaneous polarization is not abrupt but gradual (Fig. 4), suggesting that the phase transition feature should be second order, in good agreement with the DSC, HC, and dielectric permittivity measurements.

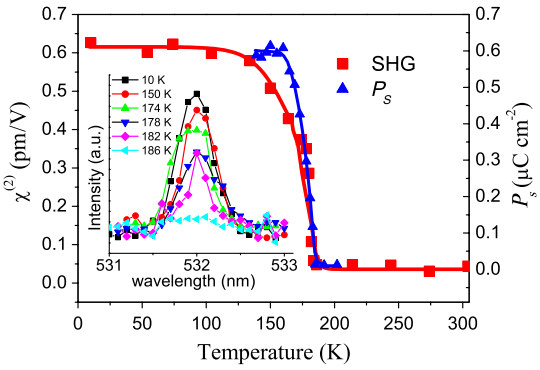

FIG. 4 (color online). The temperature dependence of the second-order nonlinear effective coefficient (left) and spontaneous polarization (right). The inset shows the intensity of SHG as function of wavelength at different temperatures.

The electric dipole contributions to SHG have been studied in many piezoelectric and ferroelectric crystals and the underlying microscopic mechanisms are well understood. SHG is very sensitive to symmetry breaking upon temperature changing because only noncentrosymmetric solid displays SHG signal. This technology is widely used in confirmation of symmetry breaking and ferroelectric domain structure. The dielectric constant can be deduced by differentiating Eq. (1) twice with respect to electric displacement D as [1]

$$1/\varepsilon = \alpha' + 3\beta' D^2 + 5\gamma' D^4, \quad (6)$$

where $D = D_E + P_s$ (D_E is electric displacement induced by the external electric field). At quasistatic frequency the nonlinear coefficients contain contributions from both the ionic and electronic polarization, while at optical frequency they contain contributions only from electronic polarization. Here, we use α', β', and γ' instead of formerly used coefficients α, β, and γ in order to emphasize these differences. The refractive index can be written as $n^2 = \varepsilon_\infty/\varepsilon_0$. Therefore, Eq. (6) is reduced as

$$\begin{aligned}\frac{1}{n^2} - \frac{1}{n_0^2} &= (6\varepsilon_0\beta' P_s + 20\varepsilon_0\gamma' P_s^3 + \cdots)D_E \\ &\quad + (3\varepsilon_0\beta' + 30\varepsilon_0\gamma' P_s^2 + \cdots)D_E^2 \\ &= \chi^{(2)}D_E + \chi^{(3)}D_E^2, \end{aligned} \quad (7)$$

where n_0 is refractive index without external electric field, and $\chi^{(2)}D_E$ and $\chi^{(3)}D_E^2$ indicate the distortion of index ellipsoid induced by electric field. At low frequencies the term $\chi^{(2)}D_E$ describes the linear (Pockels) electro-optic effect and the term $\chi^{(3)}D_E^2$ describes the quadratic (Kerr) effect. At optical frequencies these terms describe the nonlinear optical susceptibilities [1]. If ignoring the high-order terms, we get $\chi^{(2)} = 6\varepsilon_0\beta' P_s$ and $\chi^{(3)} = 3\varepsilon_0\beta'$. Since the β' is almost independent of the temperature, it is clearly shown that the behavior of the temperature dependence of the second-order nonlinear coefficient is consistent with that of P_s. The temperature dependence of SHG of CMAP is shown in Fig. 4. Above 184 K, there is no signal at the wavelength of 532 nm. However, below 184 K, a clear peak appears at the wavelength of 532 nm (inset of Fig. 4). It indicates that the structure of CMAP turns from a centrosymmetric structure above 184 K to a noncentrosymmetric one below 184 K, which is consistent with the XRD structure analysis. This linear relationship between P_s and $\chi^{(2)}$ has been observed in many displacive-type ferroelectrics, such as $LiTaO_3$, $LiNbO_3$, BTO, while order-disorder ferroelectric $NaNO_2$ seems to have no simple relationship [1], indicating that the primary contribution to the ferroelectricity of CMAP is from displacive-type.

In our sample, we assume that the positions of cations and anions are located at the protonated nitrogen atom and the chlorine ion, respectively. At 293 K, two protonated nitrogen atoms and two chlorine atoms of a unit cell are located at (0.7829, 0.25, 0.9443), (0.2171, 0.75, 0.0557), and (0.499 39, 0.25, 0.219 41), (0.500 61, 0.75, 0.780 59), respectively. Obviously, the centers of the positive and negative ions are both located at (0.5, 0.5, 0.5). Therefore, there is no any remnant electric dipole moment at 293 K [Fig. 1(d)]. However, at 93 K, the two protonated nitrogen atoms and two chlorine atoms of a unit cell are located at (0.720 13, 0.8813, 0.548 51), (0.279 87, 0.3813, 0.451 49), and (0.999 35, 0.905 08, 0.283), (0.000 65, 0.405 08, 0.717), respectively. The centers of the positive and negative ions are located at (0.5, 0.6313, 0.5) and (0.5, 0.655 08, 0.5). A remnant electric dipole moment appears along the b axis with a value of 1.49 Debye (1 Debye $= 3.3356 \times 10^{-30}$ C $\cdot$ m) [Fig. 1(c)]. The P_s of ferroelectrics can be written as

$$P_s = \lim \frac{1}{V} \sum q_i r_i. \tag{8}$$

The P_s of CMAP is 1.06 μC $\cdot$ cm^{-2}, which is very close to the values calculated from the HC (0.90 μC $\cdot$ cm^{-2}) and DSC (0.99 μC $\cdot$ cm^{-2}). The experimental results (Figs. 3 and 4) are a little smaller than that of the theoretical P_s due to some defects and dislocations of the crystal and some small deviation from the b axis, indicating that our sample is a displacive-type ferroelectric. The electric dipole moment in a unit cell of BTO is 3.18 Debye, which is about 2 times of that of our sample. On the other hand, the unit cell volume of our sample is about 7 times of that of BTO. These factors contribute to the fact that the spontaneous polarization of CMAP is much smaller than that of BTO. Furthermore, it is known that the Curie constants of displacive-type and order-disorder type ferroelectrics are generally about 10^5 K and 10^3 K [7]. However, the Curie constant of compound CMAP is only 1031 K at a frequency of 1 MHz, which locates in the range of order-disorder type ferroelectrics. One reason is that the Curie constants of organic ferroelectrics are usually smaller than that of inorganic ferroelectrics. For example, the Curie constant of $[H_2\text{-TPPZ}][Hxa]_2$, an order-disorder type ferroelectric, is only 39.5 K [18]. The Curie constants of displacive-type ferroelectrics, Phz-H_2ca and Phz-H_2ba, are 5000 K and 4000 K, respectively [19]. The Curie constant of a well-known displacive-type ferroelectric, thiourea [19], is 3700 K [7]. The Curie constant of our sample is about 1031 K, which is a little smaller than that observed in these organic displacive-type ferroelectrics and has no difference in magnitude. It is ascribed to the smaller polarization and larger molecular volume in organic ferroelectrics. Another reason is that order-disorder feature coexists with a displace feature in compound CMAP. Petzelt and Hlinka *et al.* reported that the central mode and the soft mode, which represent order-disorder feature and displacive feature, respectively, coexist in some ferroelectrics such as triglycine sulfate , SbSI, tris-sarcosine calcium chloride, and BTO [21–23]. The perchlorate of compound CMAP is disordered in high temperature while ordered in low temperature (Fig. 1).

In conclusion, we have successfully explored a new displacive-type molecule-based ferroelectric with a relatively short conversion time, which is never shown in recent documents. This simple organic salt will open up a new avenue for novel molecule-based ferroelectrics used as a FeRAM device.

This work was supported by NSFC (21071030, 20931002, and 90922005). We thank Professor X. Y. Chen and Dr. H. M. Zhu of Fujian Inst. Res. Struct. Matter, China, for their kind help with SHG measurements. X. R. G. thanks the reviewers for their excellent suggestions and Jin-Rui Lin for his synthetic work.

*zhangwen@seu.edu.cn
†xiongrg@seu.edu.cn

[1] M. E. Lines and A. M. Glass, *Principles and Applications of Ferroelectrics and Related Materials* (Oxford University Press, New York, 2001).
[2] J. F. Scott, Science **315**, 954 (2007).
[3] T. Hang, W. Zhang, H. Y. Ye, and R. G. Xiong, Chem. Soc. Rev. **40**, 3577 (2011).
[4] W. Zhang, H. Y. Ye, and R. G. Xiong, Coord. Chem. Rev. **253**, 2980 (2009).
[5] S. Brazovskii and N. Kirova, Synth. Met. **159**, 2205 (2009).
[6] N. Kirova and S. Brazovskii, Physica B (Amsterdam) **404**, 382 (2009).
[7] S. Horiuchi and Y. Tokura, Nature Mater. **7**, 357 (2008).
[8] S. Horiuchi, S. Tokunaga, G. Giovannetti, S. Picozzi, H. Itoh, R. Shimano, R. Kumai, and Y. Tokura, Nature (London) **463**, 789 (2010).
[9] M. Szafrański, A. Katrusiak, and G. J. McIntyre, Phys. Rev. Lett. **89**, 215507 (2002).
[10] W. Zhang, L. Z. Chen, R. G. Xiong, T. Nakamura, and S. P. D. Huang, J. Am. Chem. Soc. **131**, 12544 (2009).
[11] A. Katrusiak and M. Szafrański, Phys. Rev. Lett. **82**, 576 (1999).
[12] W. Zhang, H. Y. Ye, H. L. Cai, J. Z. Ge, R. G. Xiong, and S. P. D. Huang, J. Am. Chem. Soc. **132**, 7300 (2010).
[13] M. Szafrański, Phys. Rev. B **72**, 054122 (2005).
[14] M. Szafrański and A. Katrusiak, Phys. Rev. B **73**, 134111 (2006).
[15] R. Jakubas, A. Piecha, A. Pietraszko, and G. Bator, Phys. Rev. B **72**, 104107 (2005).
[16] A. Piecha, A. Pietraszko, G. Bator, and R. Jakubas, J. Solid State Chem. **181**, 1155 (2008).
[17] H. Y. Ye, D. W. Fu, Y. Zhang, W. Zhang, R. G. Xiong, and S. P. D. Huang, J. Am. Chem. Soc. **131**, 42 (2009).
[18] S. Horiuchi, R. Kumai, Y. Tokunaga, and Y. Tokura, J. Am. Chem. Soc. **130**, 13382 (2008).

[19] S. Horiuchi, F. Ishii, R. Kumai, Y. Okimoto, H. Tachibana, N. Nagaosa, and Y. Tokura, Nature Mater. **4**, 163 (2005).

[20] See Supplemental Material at http://link.aps.org/supplemental/10.1103/PhysRevLett.107.147601 for further experimental details, XRD data, IR spectra, and fitting results..

[21] J. Petzelt, G. Kozlov, and A. Volkov, Ferroelectrics **73**, 101 (1987).

[22] J. Hlinka, T. Ostapchuk, D. Nuzhnyy, J. Petzelt, P. Kuzel, C. Kadlec, P. Vanek, I. Ponomareva, and L. Bellaiche, Phys. Rev. Lett. **101**, 167402 (2008).

[23] I. Ponomareva, L. Bellaiche, T. Ostapchuk, J. Hlinka, and J. Petzelt, Phys. Rev. B **77**, 012102 (2008).